

Combining Harmonic Generation and Laser Chirping to Achieve High Spectral Density in Compton Sources

Balša Terzić,^{1,2,*} Cody Reeves,³ and Geoffrey A. Krafft^{1,2,3}

¹*Department of Physics, Old Dominion University, Norfolk, Virginia 23529, USA*

²*Center for Accelerator Science, Old Dominion University, Norfolk, Virginia 23529, USA*

³*Jefferson Lab, Newport News, Virginia 23606, USA*

Recently various laser-chirping schemes have been investigated with the goal of reducing or eliminating ponderomotive line broadening in Compton or Thomson scattering occurring at high laser intensities. As a next level of detail in the spectrum calculations, we have calculated the line smoothing and broadening expected due to incident beam energy spread within a one-dimensional plane wave model for the incident laser pulse, both for compensated (chirped) and unchirped cases. The scattered compensated distributions are treatable analytically within three models for the envelope of the incident laser pulses: Gaussian, Lorentzian, or hyperbolic secant. We use the new results to demonstrate that the laser chirping in Compton sources at high laser intensities: (i) enables the use of higher order harmonics, thereby reducing the required electron beam energies; and (ii) increases the photon yield in a small frequency band beyond that possible with the fundamental without chirping. This combination of chirping and higher harmonics can lead to substantial savings in the design, construction and operational costs of the new Compton sources. This is of particular importance to the the widely popular laser-plasma accelerator based Compton sources, as the improvement in their beam quality enters the regime where chirping is most effective.

PACS numbers: 29.20.Ej, 29.25.Bx, 29.27.Bd, 07.85.Fv

Compton or Thomson sources are increasingly being considered as potential sources of high-energy photons [1, 2]. A principal attraction of such sources is the narrow bandwidth generated in the output radiation. As a narrow bandwidth is desired, it is important to understand the sources of line width in the scattered radiation and to eliminate them to the extent possible. Recently it has been shown by a Jefferson Lab group [3] (hereafter TDHK2014) and others [4, 5] that the linewidth can be preserved against ponderomotive line broadening [6] (hereafter K2004) even at high laser intensities by proper chirping of the laser pulse.

It has been understood for many years in the FEL community [7–9] that harmonic generation can provide a path to a given radiation wavelength with a smaller electron energy than is needed for fundamental emission, or that harmonic generation provides access to shorter wavelengths for a given electron beam energy. This idea, as applied to Compton sources, suffers from the fact that whenever the field strength is low enough that ponderomotive broadening is negligible, emission into the harmonics falls off rapidly with harmonic number. On the other hand, if the field strength is large enough for substantial harmonic emission, ponderomotive broadening limits the spectral density of the emission, increasingly at high harmonic number. The main motivation for our present work is to point out how important it is that the new chirping prescriptions remove ponderomotive broadening from the harmonics, allowing high emitted spectral density in the harmonics at high field strength.

In this work we have calculated spectra for both the compensated and uncompensated cases in regimes where the normalized vector potential is of order 1, i.e. where

significant ponderomotive broadening is expected. We then use the new results to demonstrate that the laser chirping in Compton sources enables them to retain the narrowband radiation and increase the photon yield in all harmonics at high laser intensities. The increase in the photon yield enables the efficient use of higher-order harmonics, which greatly reduces the strain on the electron beam source. Combining laser chirping and the higher harmonics is particularly beneficial for the Compton sources based on the laser-plasma accelerators, as their improved beam energy spread enters the range in which the chirping is most effective.

Ponderomotive line broadening is due to the variable red-shifting of the emitted radiation because the longitudinal velocity of the electrons changes within the incident laser pulse. Compensating the local value of the frequency in the incident laser pulse against the ponderomotive longitudinal velocity change to yield constant emitted frequency through the (relativistic) Doppler shift leads to analytic expressions for the proper frequency modulation (FM) to achieve *perfect* compensation [3]. It is perfect because the bandwidth of the backscattered radiation is reduced to that of the incoming laser pulse, thereby reaching the physical limit.

Here, as in TDHK2014, calculations are completed using the formalism developed in K2004 for the far-field spectral distribution of photons Thomson-scattered by a single electron. The incident laser pulse is described by a plane wave. The treatment is fully relativistic and includes the classical electron motion without approximation. We assume a linearly polarized incident plane wave described by a single component for the normalized vector potential $\hat{A}(\xi) = eA(\xi)/mc = a(\xi) \cos(2\pi\xi f(\xi)/\lambda)$

where $a(\xi)$ describes the envelope of the oscillation, $\xi = z + ct$ is the coordinate along the laser pulse, $f(\xi)$ specifies the laser FM, and λ is a normalizing wavelength.

Expressions for backscattered radiation spectra in high-intensity Compton sources emitted by a beam with an energy spread are derived from the equations for scattering off a single electron. K2004 derives expressions for the constant-frequency laser pulses, while TDHK2014 provides the spectra for FM laser pulses.

Both derivations for the backscattered radiation spectrum $(d^2E/d\omega d\Omega)_{\text{beam}}$ start with

$$\left(\frac{d^2E(\omega)}{d\omega d\Omega}\right)_{\text{beam}} = \int_1^\infty N(\gamma) \frac{d^2E(\gamma, \omega)}{d\omega d\Omega} d\gamma, \quad (1)$$

where ω is the frequency of the scattered radiation, Ω is the solid angle of the radiation, γ is the relativistic factor, $N(\gamma)$ is the beam's energy distribution and $d^2E/d\omega d\Omega$ the radiation of a single electron. The single-electron scattering spectrum can be expressed as in TDHK2014

$$\frac{d^2E(\gamma, \omega)}{d\omega d\Omega} = \left(\frac{d^2E(\gamma)}{d\omega d\Omega}\right)_n \left(\frac{\omega}{\omega_0(\gamma)}\right)^2 \left|\frac{(1+\beta)\gamma D_x}{\lambda}\right|^2, \quad (2)$$

where $\omega_0(\gamma) = (1+\beta)^2\gamma^2 2\pi c/\lambda$ is the normalizing frequency, $(d^2E(\gamma)/d\omega d\Omega)_n = (1+\beta)^2\gamma r_e E_{\text{beam}}/c$ is the normalization factor and c the speed of light. We recast the frequency content form D_x from Eq. (7) of TDHK2014

$$\begin{aligned} \tilde{D}_x &\equiv \frac{(1+\beta)\gamma D_x(\gamma, \omega)}{\lambda} \\ &= \frac{1}{2} \int_{-\infty}^{\infty} a(\xi) \exp\left[-2\pi i \left(\xi f(\xi) + \frac{\omega}{\omega_0(\gamma)} \tilde{Z}(\xi)\right)\right] d\xi, \end{aligned} \quad (3)$$

where $\tilde{Z}(\xi) = \xi + \int_{-\infty}^{\xi} \tilde{A}^2(\xi') d\xi'$ and the FM function

$$f(\xi) = \frac{1}{1+a(0)^2/2} \left(1 + \frac{\int_0^{\xi} a(\xi')^2 d\xi'}{2\xi}\right). \quad (4)$$

Therefore, the beam energy only scales the spectrum in both frequency and amplitude:

$$\frac{d^2E(\gamma, \omega)}{d\omega d\Omega} = \left(\frac{d^2E(\gamma)}{d\omega d\Omega}\right)_n \left(\frac{\omega}{\omega_0(\gamma)}\right)^2 \left|\tilde{D}_x\left(\frac{\omega}{\omega_0(\gamma)}\right)\right|^2. \quad (5)$$

This means that for each experiment, it suffices to compute only one scale-free single-electron spectrum, $\tilde{D}_x(\omega/\omega_0)$, as in K2004 and TDHK2014. The computation of Eq. (1) is then reduced to integration of that scale-free spectrum, properly shifted and scaled. This treatment applies to both constant frequency scattering of K2004 and FM scattering in TDHK2014, and to all harmonics.

Figure 2(b) in TDHK2014 demonstrates the perfect agreement between the frequency bandwidth of the incoming laser pulse and the bandwidth of the backscattered radiation after the FM, and the near-agreement in

their maximum amplitudes. Therefore, to first order, one can approximate the first harmonic of the backscattered radiation spectrum for a FM laser pulse by its Fourier transform:

$$\tilde{D}_x\left(\frac{\omega}{\omega_0(\gamma)}\right) = \frac{1}{2} \mathcal{F}\{a(\xi)\} \left(\frac{\frac{\omega}{\omega_0(\gamma)} - \tilde{w}_f}{\tilde{w}_f}\right). \quad (6)$$

The peak width is scaled by $\tilde{w}_f = 1/(1+a_0^2/2)$ due to the first-order expansion of $\tilde{Z}(\xi)$ around $\xi = 0$ in Eq. (3). For the three laser pulse shapes considered here: Gaussian $a_G(\xi) = a_0 \exp[-\xi^2/(2(\sigma\lambda)^2)]$, Lorentzian $a_L(\xi) = a_0\sigma/((\xi/\lambda)^2 + \sigma)$ and hyperbolic secant $a_S(\xi) = a_0 \text{sech}(\sigma\xi/\lambda)$, they are:

$$\tilde{D}_{x,G}\left(\frac{\omega}{\omega_0}\right) = a_0\sigma\sqrt{\frac{\pi}{2}} \exp\left(-\frac{\left(\frac{\omega}{\omega_0} - \tilde{w}_f\right)^2}{2\tilde{\Sigma}^2}\right), \quad (7a)$$

$$\tilde{D}_{x,L}\left(\frac{\omega}{\omega_0}\right) = \frac{a_0\pi\sigma}{4} \exp\left(-\frac{\left|\frac{\omega}{\omega_0} - \tilde{w}_f\right|}{2\tilde{\Sigma}}\right), \quad (7b)$$

$$\tilde{D}_{x,S}\left(\frac{\omega}{\omega_0}\right) = \frac{a_0\pi}{2\sigma} \text{sech}\left(\frac{\pi^2}{\bar{\sigma}} \left(\frac{\omega}{\omega_0} - \tilde{w}_f\right)\right), \quad (7c)$$

where $\Sigma = 1/2\pi\sigma$, $\tilde{\Sigma} = \Sigma\tilde{w}_f$ and $\bar{\sigma} = \sigma\tilde{w}_f$. These are achieved by FM:

$$f_G(\bar{\xi}) = \tilde{w}_f \left(1 + \frac{\sqrt{\pi}\sigma a_0^2}{4\bar{\xi}} \text{erf}(\bar{\xi}/\sigma)\right), \quad (8a)$$

$$f_L(\bar{\xi}) = \tilde{w}_f \left(1 + \frac{\sqrt{\sigma}a_0^2}{4\sqrt{2}\bar{\xi}} \left(\frac{\sqrt{2}\sigma\bar{\xi}}{\sigma + 2\bar{\xi}^2} + \tan^{-1} \frac{\sqrt{2}\bar{\xi}}{\sqrt{\sigma}}\right)\right) \quad (8b)$$

$$f_S(\bar{\xi}) = \tilde{w}_f \left(1 + \frac{a_0^2}{2\bar{\xi}\sigma} \tanh(\sigma\bar{\xi})\right), \quad (8c)$$

with $\bar{\xi} = \xi/\lambda$.

Obtaining an analytic approximation for the shape of the higher-order harmonics in the FM spectrum requires a derivation similar to that in [10]. After substituting Eq. (4) into Eq. (3), integrating by parts, using $\exp(i\alpha \sin \theta) = \sum_{n=-\infty}^{\infty} J_n(\alpha) \exp(in\theta)$, where J_n is the Bessel function of the n th order, and expanding around the stationary phase point, we find the contribution of the n th harmonic to the scale-free spectrum $\tilde{D}_x = \sum_n \tilde{D}_x^n$

$$\tilde{D}_x^n = \int_0^\infty a(\xi) K_n(g(\xi)) \cos(2\pi Z(\xi)\bar{\omega}_n) d\xi, \quad (9)$$

with $K_n(\alpha) = (-1)^n [J_n(\alpha) - J_{n-1}(\alpha)]$, $g(\xi) = a^2(\xi)(n-1/2)/(2(1+1/2a^2(\xi)))$, $\bar{\omega}_n = \omega/\omega_0 - 2(n-1/2)\tilde{w}_f$ and $Z(\xi) = \xi + (1/2)\int_0^\xi a^2(\xi') d\xi'$. Examining $K_n(g(\xi))$, an implicit function of ξ , reveals that the explicit function $\tilde{K}_n(\xi)$ is well-approximated by a Gaussian $\tilde{K}_n(\xi) \approx A_n \exp(-\xi^2/2\Sigma_n)$ for $n > 1$ and a shifted Gaussian $\tilde{K}_1(\xi) \approx 1 + A_1 \exp(-\xi^2/2\Sigma_1)$ for

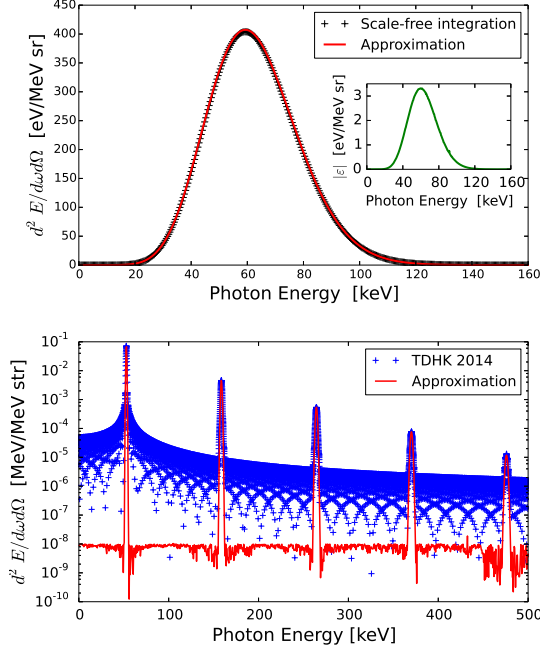


FIG. 1: Spectra from scattering a FM Gaussian laser pulse with $\lambda = 800$ nm, $a_0 = 0.587$ off a Gaussian electron beam with $Q = 100$ pC and $E_0 = 51.1$ MeV. (a) Integration of a single scale-free spectrum \tilde{D}_x and an electron beam with a 34% energy spread versus the approximation from Eq. (13a) (red line). The inset shows the absolute difference ϵ between the two results. (b) Single-electron scattering approximation in Eq. (10) against the exact solution of TDHK2014.

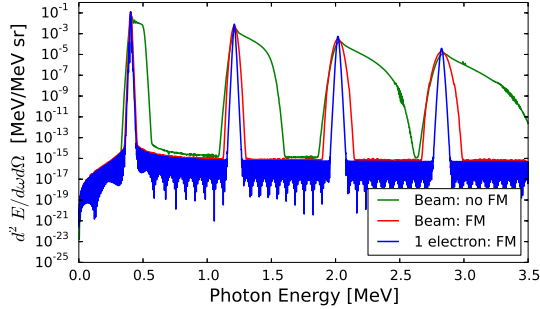


FIG. 2: Backscattered radiation of a Gaussian laser pulse with $\lambda = 1$ μm , $a_0 = 0.707$ off a Gaussian electron beam with $Q = 100$ pC, $E_0 = 163$ MeV, and 1% FWHM energy spread: FM (red), non-FM (green), and the single electron FM case (normalized to FM) (blue). Lorentzian and hyperbolic secant behave similarly.

$n = 1$, where $A_1 = K_1(g(0)) - 1$, $A_n = K_n(g(0))$, $\Sigma_1 = \sqrt{-B_1^2/2 \log((B_1 - 1)/A_1)}$, $\Sigma_n = \sqrt{-B_n^2/2 \log(B_n/A_n)}$, $B_n = K_n(g(\sigma))$. Keeping only the linear term in $Z(\xi)$, we obtain analytic approximation for all harmonics:

$$\begin{aligned} \tilde{D}_x^1 &= \frac{1}{2} \mathcal{F} \left\{ a(\xi) \left(1 + A_1 \exp \left[-\frac{\xi^2}{2\Sigma_1^2} \right] \right) \right\} \left(\frac{\bar{\omega}_1}{\tilde{w}_f} \right) \quad (10a) \\ \tilde{D}_x^n &= \frac{1}{2} \mathcal{F} \left\{ a(\xi) A_n \exp \left[-\frac{\xi^2}{2\Sigma_n^2} \right] \right\} \left(\frac{\bar{\omega}_n}{\tilde{w}_f} \right). \quad (10b) \end{aligned}$$

Neglecting a correction due to the small parameter A_1 , the result for the leading-order harmonic in Eq. (6) is recovered. An excellent agreement between this approximation and the exact scale-free solution is shown in Fig. 1(a). For the higher-order harmonics, only Gaussian pulse yields an analytic approximation, shown in Fig. 1(b). The agreement is nearly perfect. The Eq. (10) suggests that only for the Gaussian laser pulse is the shape of all the harmonics the same. The higher-order harmonics of the Lorentzian and hyperbolic secant pulse are different from their respective first harmonics.

The maximum amplitude of the harmonics is computed from Eq. (10) by substituting $\int_{-\infty}^{\infty} d\xi$ for $\mathcal{F}\{\}$:

$$\left| \tilde{D}_x^{1,n} \right|_{\max,G} = a_0 \sqrt{\frac{\pi}{2}} (\sigma + A_1 s_G^1, A_n s_G^n), \quad (11a)$$

$$\left| \tilde{D}_x^{1,n} \right|_{\max,L} = a_0 (\pi\sqrt{\sigma} + A_1 s_L^1, A_n s_L^n), \quad (11b)$$

where $s_G^n = \sigma \Sigma_n / \sqrt{\Sigma_n^2 + \sigma^2}$, $s_L^n = (\pi/2\sqrt{\sigma}) \exp(\beta_n^2) [1 - \text{erf}(\beta_n)]$ and $\beta_n = \sqrt{\sigma/2\Sigma_n^2}$. The width of the harmonics for the Gaussian pulse are

$$W_G^1 \approx \frac{\tilde{w}_f}{2\pi\sigma}, \quad W_G^n = \frac{\tilde{w}_f}{2\pi s_G^n}. \quad (12)$$

For FWHM in eV, these are multiplied by $2.35\hbar\omega_0$.

For the Gaussian electron beam distribution and the case with FM, substituting Eq. (7) into Eq. (5) and Eq. (1) leads to analytic solutions after invoking a well-justified approximation that the narrowband backscattered radiation off a single electron $d^2 E(\gamma, \omega)/d\omega d\Omega$ is highly peaked around $\bar{\gamma}(\omega) = \sqrt{\lambda\omega/2\pi c\tilde{w}_f}$. Then the single-electron spectra are well-approximated by a Gaussian, which exactly integrates into analytic expressions for the leading-order harmonic:

$$\left(\frac{d^2 E(\omega)}{d\omega d\Omega}\right)_{\text{beam,FM,G}} = \frac{Qer_e a_0^2 \sigma^2 \lambda \tilde{w}_f}{4q_e c^2} \frac{S_G(\omega)\omega}{\sqrt{\tilde{\sigma}_E^2 + S_G(\omega)^2}} \exp\left[-\frac{(\gamma_0 - \bar{\gamma}(\omega))^2}{2(\tilde{\sigma}_E^2 + S_G^2(\omega))}\right], \quad (13a)$$

$$\left(\frac{d^2 E(\omega)}{d\omega d\Omega}\right)_{\text{beam,FM,L}} = \frac{Qer_e a_0^2 \sigma^2 \lambda \tilde{w}_f \pi^3}{32\sqrt{2}q_e c^2 \tilde{\sigma}_E} [r_+ (1 - \text{erf}(s_+)) - r_- \text{erfi}(s_-)], \quad (13b)$$

$$\left(\frac{d^2 E(\omega)}{d\omega d\Omega}\right)_{\text{beam,FM,S}} = \frac{Qer_e a_0^2 \lambda \tilde{w}_f \pi k}{8q_e c^2 \sigma^2} \frac{S_S(\omega)\omega}{\sqrt{\tilde{\sigma}_E^2 + S_S(\omega)^2}} \exp\left[-\frac{(\gamma_0 - \bar{\gamma}(\omega))^2}{2(\tilde{\sigma}_E^2 + S_S^2(\omega))}\right], \quad (13c)$$

where $S_G(\omega) = \bar{\gamma}(\omega)\Sigma/(2\sqrt{2}\tilde{w}_f)$, $S_L(\omega) = \bar{\gamma}(\omega)/(\sqrt{2\pi}\tilde{w}_f(2\sigma)^{1/4})$, $S_S(\omega) = \bar{\gamma}(\omega)\sigma/(2\sqrt{2}\pi^2\tilde{w}_f)$, $k = 1.12841$ is the normalization factor, erfi the complex error function $\text{erfi}(x) = i\text{erf}(ix)$ and

$$r_{\pm} = \frac{\exp\left[\frac{-\gamma_0^2}{2(\tilde{\sigma}_E^2 \pm S_L^2)} \mp 2\sqrt{2}\sigma\pi\tilde{w}_f\right]}{\sqrt{\tilde{\sigma}_E^2 \pm S_L^2}}, s_{\pm} = \frac{\bar{\gamma}\tilde{\sigma}_E \pm S_L^2(\bar{\gamma} - \gamma_0)}{\sqrt{2}\tilde{\sigma}_E S_L \sqrt{\tilde{\sigma}_E^2 \pm S_L^2}}.$$

A single-electron scattering is recovered when $\tilde{\sigma}_E \rightarrow 0$ and $Q = q_e$ are substituted. Figure 1(a) shows an excellent agreement between the analytic approximation Eq. (13a) and the numerical integration of Eq. (1) with a single scale-free spectrum \tilde{D}_x given in Eq. (3). The accuracy for other laser pulse shapes is similarly high. Clearly, one can confidently use either of these methods for the FM laser pulses—direct scale-free numerical integration or the analytic approximation. However, for the constant-frequency laser pulses for which the single-electron scattering $d^2 E(\gamma, \omega)/d\omega d\Omega$ can only be numerically computed as in K2004, only the scale-free integration works.

Figure 2 shows the spectrum of the backscattered radiation from a electron beam with a 1% energy spread with and without FM, and from a single-electron scattering. Clearly, the FM is still quite effective in restoring the narrowband spectrum for all harmonics simultaneously.

The bandwidth of the backscattered radiation—for both the FM and constant-frequency laser pulse—is affected by: (1) the intrinsic bandwidth of the single-electron scattering (which depends on the length of the laser pulse σ); and (2) the energy spread of the electron beam distribution, σ_E . When the electron beam energy spread is small, the bandwidth is dominated by the intrinsic single-electron scattering bandwidth. When the electron beam energy spread is high, electron beam's bandwidth dominates, thereby diminishing the effects of the FM. This is illustrated in Fig. 3.

A compensated narrow n th harmonic peaks near $E = 4\gamma^2 E_p n / (1 + (1/2)a_0^2)$, where E_p is the energy of the laser pulse. This means that a desired radiation can be achieved either by using the first harmonic from a backscattering off an electron beam with the energy $\gamma m_e c^2$, or the n th harmonic from a backscattering off an electron beam with energy $\gamma m_e c^2 / \sqrt{n}$. Such a $1/\sqrt{n}$ reduction in the required electron beam energy would lead

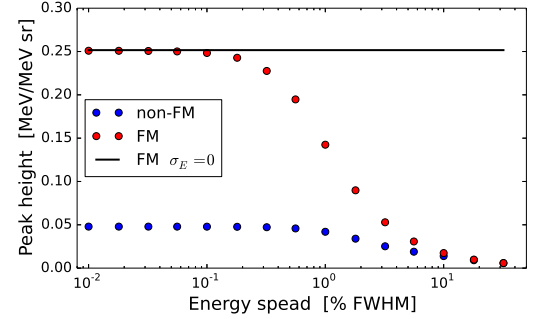


FIG. 3: Maximum amplitude as a function of the energy spread for a Gaussian laser pulse with $\lambda = 1 \mu\text{m}$, $a_0 = 0.707$ off a Gaussian electron beam with $Q = 100 \text{ pC}$, $E_0 = 163 \text{ MeV}$ without FM (blue dots) and with FM (red dots), along with the theoretical limit for the FM monochromatic ($\sigma_E = 0$) beam from Eq. (13a) (solid black line), computed by scale-free integration. The results for the Lorentzian and hyperbolic secant are virtually identical.

to substantial savings in the construction and shielding cost of the electron source.

Figure 4 summarizes the importance of FM in Compton sources. FM increases the yield in all harmonics to the point where for a high enough intensity, the power in the higher harmonics exceeds that of the non-FM first harmonic. For energy considered in this figure, 163 MeV, and the energy spread of 0.1% this occurs around $a_0 = 1$ (intensity of $1.4 \times 10^{18} \text{ W/cm}^2$) for the third FM harmonic and around $a_0 = 1.5$ ($3.1 \times 10^{18} \text{ W/cm}^2$) for the fifth FM harmonic. These translate in $\sqrt{3}$ and $\sqrt{5}$ reduction in electron beam energies, respectively. As laser-plasma accelerator performance in the sub-1% range in energy spread becomes realistic [11], using the FM higher order harmonics is poised to reap substantial benefits.

In this letter a novel calculation prescription is used to determine the emission characteristics of the scattered radiation in a Compton backscatter source. When compensated by laser beam FM the radiation line heights and widths may be accurately computed using a stationary phase argument with crisp functional forms. The calculations accurately account for detuning of the emitted radiation by beam energy spread.

Our calculations suggest the following main conclusion:

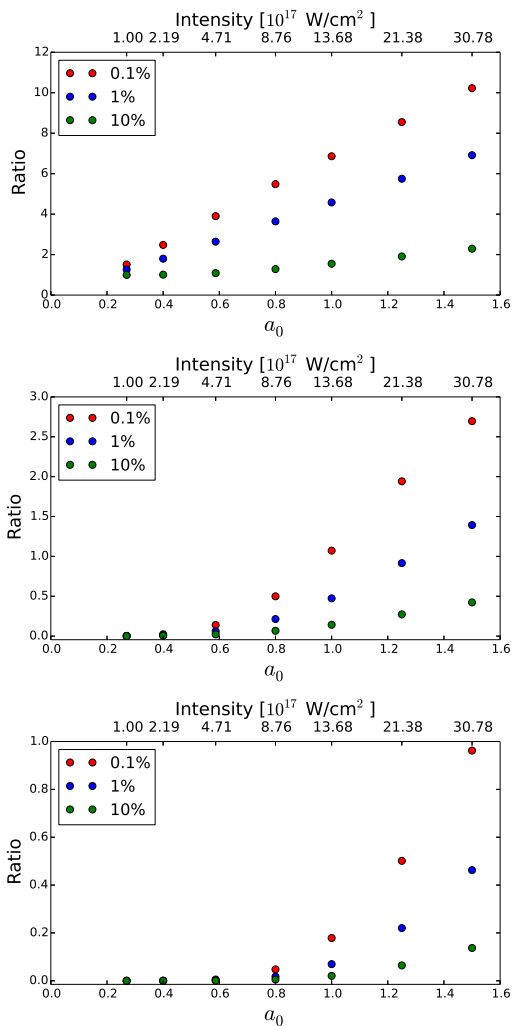


FIG. 4: Ratio of the maximum amplitudes as a function of the intensity (and the amplitude of the normalized vector potential a_0) for a Gaussian laser pulse with $\lambda = 1 \mu\text{m}$ off a Gaussian electron beam with $Q = 100 \text{ pC}$, $E_0 = 163 \text{ MeV}$ and 0.1% FWHM energy spread (red dots), 1% (blue) and 10% (green). (a) FM first harmonic divided by the non-FM first harmonic. (b) FM third harmonic divided by the non-FM first harmonic. (c) FM fifth harmonic divided by the non-FM first harmonic. The leftmost set of points ($a_0 = 0.27$ or $I = 10^{17} \text{ W/cm}^2$) corresponds to the current upper limit of operation of the laser-plasma accelerators [11].

by combining harmonic generation and frequency modu-

lation (chirping) of the incident laser pulse it should be possible to generate significant fluxes of Compton scattered radiation on the harmonic frequencies. The beam energy spread in laser-plasma acceleration schemes are becoming good enough, nearing the 1% level [11], that the energy flux density on the harmonics can even exceed that possible when an unmodulated incident laser pulse is used.

Using higher harmonics at low laser intensities the photon yield is substantially smaller than that in the first harmonic. The yield of the higher harmonics can be improved—absolutely and relatively compared to the first harmonic—by increasing the laser intensity. However, increasing the laser intensity leads to the ponderomotive broadening which erases any advantages thus incurred. Frequency modulation and its perfect restoration of the narrowband emission, becomes crucial: it mitigates the adverse effects of the ponderomotive broadening, allowing one to continue increasing the photon yield.

C. R. acknowledges the support from the U.S. Department of Energy, Science Undergraduate Laboratory Internship (SULI) program.

* Email: bterzic@odu.edu

- [1] G. A. Krafft and G. Priebe, *Rev. Accl. Sci. Tech.* **03**, 147 (2010).
- [2] Z. Huang and R. Ruth, *Phys. Rev. Lett.* **80**, 976 (1998). See also www.lynceantech.com.
- [3] B. Terzić, K. Deitrick, A. Hofer and G. A. Krafft, *Phys. Rev. Lett.* **112**, 074801 (2014).
- [4] I. Ghebregziabher, B. A. Shadwick, and D. Umstadter, *Phys. Rev. ST-AB* **16**, 030705 (2013). See also arXiv:1204.1068.
- [5] D. Seipt, S. G. Rykovanov, A. Surzhykov and S. Fritzsche, *Phys. Rev. A* **91**, 033402 (2015). See also arXiv:1412.2659.
- [6] G. A. Krafft, *Phys. Rev. Lett.* **92**, 204802 (2004).
- [7] J. M. J. Madey, *Nuovo Cimento* **B 50**, 64 (1970).
- [8] W. B. Colson, *IEEE Jour. of Quantum Electronics* **QE-17**, 1417 (1981).
- [9] S. V. Benson and J. M. J. Madey, *Phys. Rev. A* **39**, 1579 (1989).
- [10] C. Brau, *Phys. Rev. ST-AB* **7**, 020701 (2004).
- [11] C. Geddes *et al.*, *Num. Inst. Meth. B* **350**, 116 (2015).